Title
Altered brain diffusion tensor imaging indices in adolescents with the Fontan palliation

Journal
Neuroradiology, 61(7)

ISSN
0028-3940

Authors
Singh, Sadhana
Roy, Bhaswati
Pike, Nancy
et al.

Publication Date
2019-07-01

DOI
10.1007/s00234-019-02208-x

Peer reviewed

HHS Public Access
Author manuscript
Neuroradiology. Author manuscript; available in PMC 2020 July 01.

Published in final edited form as:
Neuroradiology. 2019 July ; 61(7): 811–824. doi:10.1007/s00234-019-02208-x.

Altered Brain Diffusion Tensor Imaging Indices in Adolescents with the Fontan Palliation

Sadhana Singh, PhD[1,*], **Bhaswati Roy, PhD**[2,*], **Nancy Pike, PhD**[2], **Ebenezer Daniel, PhD**[1], **Luke Ehlert, BS**[1], **Alan B. Lewis, MD**[3], **Nancy Halnon, MD**[4], **Mary A. Woo, PhD**[2], and **Rajesh Kumar, PhD**[5,6]

[1]Department of Anesthesiology, David Geffen School of Medicine at UCLA, University of California at Los Angeles, 56-141 CHS, 10833 Le Conte Aves, Los Angeles, CA, 90095-1763, USA.

[2]UCLA School of Nursing, University of California Los Angeles, Los Angeles, CA, USA.

[3]Division of Cardiology, Children's Hospital, Los Angeles, CA, USA.

[4]Division of Pediatric Cardiology, University of California Los Angeles, Los Angeles, CA, USA.

[5]Department of Anesthesiology, David Geffen School of Medicine at UCLA, University of California at Los Angeles, 56-141 CHS, 10833 Le Conte Aves, Los Angeles, CA, 90095-1763, USA.

[6]Department of Radiological Sciences, University of California Los Angeles, Los Angeles, CA,

Abstract

Purpose: Single ventricle heart disease (SVHD) patients show injury in brain sites that regulate autonomic, mood, and cognitive functions. However, the nature (acute or chronic changes) and extent of brain injury in SVHD are unclear. Our aim was to examine regional brain tissue damage in SVHD over controls using DTI-based mean diffusivity (MD), axial diffusivity (AD), radial diffusivity (RD), and fractional anisotropy (FA) procedures.

Methods: We collected two DTI series (3.0–Tesla MRI), mood and cognitive data from 27 SVHD and 35 control adolescents. Whole-brain MD, AD, RD, and FA maps were calculated from each series, realigned and averaged, normalized to a common space, smoothed, and compared between groups using ANCOVA (covariates, age and sex; false-discovery-rate, $p<0.05$). Region-

Addresses for Correspondence: Rajesh Kumar, PhD, Department of Anesthesiology, 56-141 CHS, 10833 Le Conte Aves, David Geffen School of Medicine at UCLA, University of California at Los Angeles, Los Angeles, CA 90095-1763, USA, Tel: 310-206-1679, 6133, Fax: 310-825-2236, rkumar@mednet.ucla.edu.
*= Equal contribution

Conflict of Interest: The authors declare that they have no conflict of interest.

Ethical approval: All procedures performed in studies involving human participants were in accordance with the ethical standards of the institutional research committee.

Informed consent: Informed consent was obtained from all individual participants included in the study.

of-interest analyses were performed to calculate MD, AD, RD, and FA values for magnitude assessment between groups.

Results: SVHD patients showed impaired mood and cognitive functions over healthy adolescents. Multiple brain sites in SVHD showed increased MD values, including the insula, caudate, cingulate, hypothalamus, thalamus, medial prefrontal and frontal cortices, para-hippocampal gyrus, hippocampus, precentral gyrus, amygdala, cerebellum, corpus callosum, basal-forebrain, mammillary bodies, internal capsule, midbrain, fornix, and occipital, parietal, and temporal cortices, indicating chronic tissue changes. Similar areas showed either increased AD or RD values, with RD changes more enhanced over AD in SVHD compared to controls. Few brain regions emerged with increased or decreased FA values in SVHD patients over controls.

Conclusions: SVHD adolescents, more than a decade from their last surgical procedure, show widespread brain abnormalities in autonomic, mood, and cognitive regulatory areas. These findings indicate that brain injury is in a chronic stage in SVHD with predominantly myelin changes that may result from previous hypoxia/ischemia- or developmental-induced processes.

Keywords

Single ventricle heart disease; diffusion tensor imaging; cognition; brain injury

INTRODUCTION

Single ventricle heart disease (SVHD) is a subgroup of complex congenital heart disease that typically requires three staged palliative heart surgeries at a young age with the culmination being the Fontan procedure. Adolescents with SVHD show brain tissue injury [1–3], in particular gray and white matter damage in sites that regulate autonomic, mood, and cognitive functions, which are commonly deficient in the condition. Various magnetic resonance imaging (MRI) procedures, including the diffusion tensor imaging (DTI)-based fractional anisotropy (FA), have been used to assess brain tissue changes in SVHD adolescents. Lower FA values have shown in multiple white matter (WM) areas in infants and adolescents with congenital heart disease [1,3]. Although FA measures are known to be highly sensitive for identification of microstructural tissue changes, the procedures are not very specific for determination of nature (e.g., acute or chronic) and types of brain changes (e.g., axonal or myelin changes). Decreased FA values are reported in both acute, as well as in chronic conditions in patients with liver failure [4] and optic neuritis [5]. Thus, the nature (whether acute or chronic tissue changes) and types (axonal or myelin changes) of brain injury at the microstructural level in SVHD subjects are unclear. Other DTI indices, including mean diffusivity (MD), and axial diffusivity (AD) and radial diffusivity (RD) can determine nature and types of brain injury more precisely in SVHD adolescents.

Using DTI data, along with FA, several other DTI measures, including the MD, AD, and RD indices can be calculated and may be helpful to examine tissue changes. Mean diffusivity measures the average motion of water molecules within the tissue and shows reduced values in acute and increased values in chronic condition [6–8]. In addition, AD measures water diffusion parallel to fibers and indicates axonal changes, and RD assesses water diffusion perpendicular to fibers and shows myelin changes [9]. Multiple studies, including those examining multiple sclerosis [10], Alzheimer disease [11], traumatic brain injury [12], obstructive sleep apnea [13], heart failure [14], and congenital central hypoventilation syndrome [15] have successfully used MD, AD, and RD procedures to characterize the nature and types of brain microstructural changes, and thus, may be useful in SVHD adolescents for such assessment.

Our aim was to examine the nature and types of tissue injury in the same brain sites in adolescents with SVHD who have undergone surgical palliation with Fontan completion compared to healthy adolescents using MD, AD, RD, and FA procedures. We hypothesized that SVHD adolescents will show increased MD values and predominantly higher AD, and RD values, and altered FA values over healthy control subjects in brain areas that regulate autonomic, mood, and cognitive functions.

METHODS

Study Sample

We studied 62 adolescents which include 27 SVHD and 35 controls. Demographic and clinical data for SVHD and control subjects are summarized in Table 1. Single ventricle heart disease participants (age range, 14–18 years), who have undergone surgical palliation with Fontan completion, were recruited via flyers or provider referrals from the University Hospital and pediatric cardiology clinics. Control subjects were screened as healthy with no medical or psychiatric disorders, taking no medications, or history of previous head injury (e.g. concussions, trauma) and were recruited from the local community. Exclusion criteria for SVHD and control adolescents were claustrophobia, non-removable metal (such as dental braces, pacemakers), developmental delay precluding active study participation or ability for self-report (e.g. cerebral palsy or severe hypoxic-injury), diagnosis of depression, premature birth (< 37 weeks gestation), history of extracorporeal membrane oxygenation (ECMO) use, stroke, and cardiac arrest. Clinical and demographic details of SVHD and controls were collected from self-report and medical records. The study was approved by the Institutional Review Board. Parental permission and assent were obtained for participants under 18 years, and informed consents were obtained from participants over 18 years before data collection.

Assessment of Depression and Anxiety

Anxiety and depressive symptoms were assessed in all subjects using self-reported questionnaires, the Beck Anxiety Inventory (BAI) [16], and the Patient Health Questionnaire-9 (PHQ–9) [17], respectively. The BAI score ranges from 0–63 based on symptom severity, and more than 9 is considered with anxiety symptoms [16]. Similarly, the PHQ–9 score ranges from 0–27, and scores from 5–9, 10–14, 15–19, and > 20 are considered with minimal, moderate, moderately-severe, and severe depressive symptoms, respectively [17].

Cognition Assessment

The Montreal Cognitive Assessment (MoCA) test, which is used to screen various cognitive domains, including attention and concentration, executive functions, language, memory, visuoconstructional skills, conceptual thinking, calculations and orientation [18], was administered in all SVHD and control subjects. The global MoCA score ranges from 0–30, and a score of < 26 is considered abnormal. Although the MoCA test is a screening tool, this instrument has been validated in adolescents and young adults with CHD [19] and showed 95% agreement with standard cognition test.

We also administered the Wide Range Assessment of Memory and Learning, 2nd Edition (WRAML2) in SVHD and controls for assessment of memory and learning functions. The WRAML2 measures various domains of memory, including the verbal and visual memory, attention/concentration, working memory, and visual and verbal recognition. The core battery consists of six subtests: story memory, verbal learning, design memory, picture memory, short-term memory of a visual sequential pattern, and numbers/letters that combined to yield a general memory index (GMI) score. Additionally, the other subtests include working memory and memory recognition and yield the general memory recognition index (GRI) score. A score of < 85 in either measurement is considered abnormal [20].

Magnetic Resonance Imaging

Brain imaging studies were performed using a 3.0–Tesla MRI scanner (Siemens, Magnetom Prisma, Erlangen, Germany). Foam pads were used on both sides of the head to minimize head motion during data acquisition. High-resolution T1-weighted images were collected using a MPRAGE pulse sequence (TR = 2200 ms; TE = 2.4 ms; inversion time = 900 ms; flip angle = 9°; matrix size = 320×320; FOV = 230×230 mm; slice thickness = 0.9 mm; number of slices = 192). Proton density (PD) and T2 weighted images [TR = 10,000 ms; TE1, 2 = 17, 134 ms; flip angle = 130°] were also acquired simultaneously using a dual-echo turbo spin-echo pulse sequence in the axial plane, with a 256×256 matrix size, 230×230 mm FOV, 3.5 mm slice thickness, and no inter-slice gap. DTI data were collected using a single-shot echo planar imaging with twice-refocused spin-echo pulse sequence (TR = 12,200 ms; TE = 87 ms; flip angle = 90°; bandwidth = 1,345 Hz/pixel; matrix size = 128×128; FOV = 230×230 mm; slice thickness = 1.7 mm, diffusion values = 0 and 800 s/mm^2, diffusion directions = 30, separate series = 2). The parallel imaging technique, generalized auto-calibrating partially parallel acquisition (GRAPPA), with an acceleration factor of two, was used for all MRI data collection.

Clinical evaluation

High-resolution T1–weighted, PD- and T2-weighted images of all SVHD and controls were examined by a neuroradiologist blinded to group assignment for any visible brain tissue pathology, such as tumors, cysts, or any other major mass lesions. These findings are tabulated in Table 2.

Data Processing

The statistical parametric mapping package SPM12 (http://www.fil.ion.ucl.ac.uk/spm/), Diffusion Toolkit [21], MRIcroN, and MATLAB-based (http://www.mathworks.com/) custom software were used for data processing and analyses, as well as visualization. Diffusion and non-diffusion weighted images of all SVHD and controls were also assessed for any head-motion related or other imaging artifacts before MD, AD, and RD calculations.

MD, AD, RD, and FA calculation—To determine diffusion tensor matrices using the Diffusion Toolkit software [21], we used diffusion-weighted ($b = 800\ s/mm^2$) and non-diffusion weighted images ($b = 0\ s/mm^2$). The diffusion tensor matrices were diagonalized, and principal eigenvalues (λ1, λ2, and λ3) were calculated [6]. These principal eigenvalues were used to calculate MD [$\lambda = (\lambda1 + \lambda2 + \lambda3)/3$], AD ($\lambda_{\parallel} = \lambda1$), RD [$\lambda_{\perp} = (\lambda2 + \lambda3)/2$], and FA $\left[\sqrt{\frac{3\left[(\lambda1-\lambda)^2+(\lambda2-\lambda)^2+(\lambda3-\lambda)^2\right]}{2\left(\lambda1^2+\lambda2^2+\lambda3^2\right)}}\right]$ values at each voxel [22,6], with voxel intensities on the MD, AD, RD, and FA maps showing the corresponding diffusion values. A fixed threshold value was used to mask-out background noise on MD, and FA maps in Diffusion Toolkit software. For AD and RD maps, non-brain regions were suppressed in all participants using individual brain masks created from non-diffusion weighted images using the SPM12 software.

Averaging, normalization, and smoothing—We used the MATLAB-based SPM12 software for pre-processing of the MD, AD, RD, and FA maps. Firstly, the MD, AD, RD, and FA maps, derived from each DTI series, were realigned to remove any potential variation from head motion and averaged. Similarly, non-diffusion weighted images were also realigned and averaged. The averaged MD, AD, RD, and FA maps were normalized to Montreal Neurological Institute (MNI) space. Non-diffusion weighted (b0) images were normalized to MNI space using a unified segmentation approach [23], and the resulting normalization parameters were applied to corresponding MD, AD, RD, and FA maps. The normalized MD, AD, RD, and FA maps were smoothed with a Gaussian filter (8 mm).

Background image—MATLAB-based SPM12 software was used to generate background image. High-resolution T1-weighted images of all SVHD and controls were normalized to the MNI space template. The normalized images were averaged to create a mean anatomical image, which was used as a background image for anatomical identification.

Statistical Analyses

We used the statistical package for social sciences (SPSS v24) for assessment of demographic and clinical data. The numerical demographic data between groups were compared with independent samples t-tests, and categorical characteristics were compared using the Chi-square test. Statistical threshold values of $p<0.05$ were considered as significant differences.

For regional brain MD, AD, RD, and FA differences between groups, the smoothed MD, AD, RD, and FA maps were compared voxel-by-voxel using ANCOVA (SPM12; covariates, age and sex; false discovery rate, $p<0.05$). The statistical parametric maps showing brain sites with significant MD, AD, RD, and FA differences between groups were superimposed onto the mean anatomical image for structural identification using MRIcroN software.

Region of interest (ROI) and Percentage (%) change Analyses

Region of interest analyses were performed to calculate MD, AD, RD, and FA values to determine magnitude differences between groups. Regional brain masks were created based on significant whole-brain voxel-by-voxel MD, AD, RD, and FA differences between groups for those regions, and values were extracted using these regional brain masks and smoothed MD, AD, RD, and FA maps of SVHD and controls with MATLAB-based custom software. To calculate percentage change in AD or RD values for each region, we subtracted the AD or RD values of SVHD from control subjects and divided by AD or RD values of control subjects.

RESULTS

Demographic and Clinical Characteristics

Demographic and clinical variables of SVHD and controls are presented in Table 1. No significant differences in age ($p = 0.44$), sex ($p = 0.75$), body mass index (BMI) ($p = 0.62$), or handedness ($p = 0.45$) appeared between groups. The majority of SVHD participants had a single right ventricle (67%), extra-cardiac Fontan procedure (78%) and were over a decade from their last surgical procedure. The PHQ-9 and BAI scores were significantly higher in SVHD over controls (PHQ–9, $p = 0.005$; BAI, $p < 0.001$). The global MoCA scores and majority of sub-scales were significantly reduced in SVHD compared to controls ($p < 0.05$). The GMI and GRI scores were significantly reduced in SVHD over controls ($p < 0.001$).

Clinical Evaluation

Brain changes based on visual examination by a neuroradiologist are outlined in Table 2. These changes in SVHD subjects included the cystic focus in right pterygoid space, periventricular white matter changes, Rathke's cleft cyst, tissue loss with encephalomalacia, lacunar infarcts, ischemic changes, and Chiari I malformation.

Regional Brain MD Changes

Multiple brain regions showed significantly increased MD values, indicating chronic tissue injury in SVHD over controls, controlling for age and sex. No brain sites emerged with decreased MD values, showing acute tissue changes, in the SVHD group compared to controls. Brain sites that showed increased MD values in the SVHD group included, bilateral insular cortices (Fig.1a), caudate nuclei (Fig.1b), anterior (Fig.1f), mid (Fig. 1g), and posterior (Fig.1c) cingulate cortices, midbrain (Fig.1d), hypothalamus (Fig.1e), fornix (Fig. 1h), bilateral mid-corona radiata (Fig.1i), parietal cortices (Fig.1j), bilateral thalamus (Fig. 1k), medial prefrontal (Fig.1l), bilateral para-hippocampal gyrus (Fig.1m), bilateral hippocampus (Fig.1n), bilateral precentral gyrus (Fig.1o), bilateral frontal gyrus (Fig.1p), bilateral amygdala (Fig.1q), cerebellar cortices (Fig.1r), occipital cortices (Fig.1s), corpus callosum (Fig.1t), bilateral basal forebrain (Fig.1u), bilateral prefrontal cortices (Fig.1v), bilateral mammillary bodies (Fig.1w), bilateral internal capsule, bilateral temporal cortices, and cerebellar vermis.

Regional Brain AD and RD Values

Axial diffusivity and RD values were significantly increased in multiple brain regions in SVHD subjects (Fig. 2). These areas included the insular cortices, caudate nuclei, occipital cortices, anterior, mid, and posterior cingulate cortices, hypothalamus, mid-corona radiata, parietal cortices, thalamus, medial prefrontal, para-hippocampal gyrus, hippocampus, precentral gyrus, frontal gyrus, amygdala, cerebellar cortices, corpus callosum, basal forebrain, prefrontal cortices, mammillary bodies, internal capsule, midbrain, fornix, temporal cortices, and cerebellar vermis (Fig.2).

Regional Brain FA Values

Fractional anisotropy values were significantly decreased in few brain regions, including the corpus callosum (Fig.3a), hippocampus (Fig.3b), anterior insula (Fig.3c), amygdala (Fig.3d), caudate, thalamus, and anterior cerebellar peduncle in SVHD patients over control subjects. Other brain regions, such as the posterior insula (Fig.3e), putamen (Fig.3f), prefrontal cortex (Fig.3g), cerebellar cortices (Fig.3h), and posterior cerebellar peduncle (Fig.3i) showed increased FA values in SVHD over controls.

ROI Analysis

Regional brain MD, AD, RD, and FA values of SVHD and control subjects are tabulated in Tables 3–6. Brain regional diffusivity values, including MD, AD, and RD, were significantly increased in SVHD compared to controls. However, FA values were significantly increased or decreased in SVHD over controls. ROI analyses showed larger RD (5–27%) changes over AD (5–18%) in most of the white matter regions in SVHD compared to controls, indicating predominantly myelin tissue changes.

DISCUSSION

SVHD patients showed chronic brain tissue injury in multiple areas that included the insula, caudate nuclei, cingulate, hypothalamus, corona radiata, thalamus, medial prefrontal and prefrontal cortices, para-hippocampal gyrus, hippocampus, precentral gyrus, amygdala, cerebellar cortices, corpus callosum, basal forebrain, mammillary bodies, internal capsule, midbrain, fornix, occipital, parietal, frontal and temporal cortices. The majority of brain areas showed more RD over AD values, indicating predominantly myelin changes in SVHD over controls. These sites are involved in autonomic, mood, and cognition functions that are adversely affected in SVHD patients. These finding may result from developmental or innate brain changes or hypoxia/ischemia injury in the condition.

Multiple neuroimaging studies have shown brain gray and white matter injury in several sites in SVHD before and after surgery [2,24]. In this study, widespread brain changes were observed in AD, RD, and MD values; however, limited sites appeared with either increased or reduced FA values in SVHD patients over controls. Few DTI based FA studies also revealed several compromised white matter areas in infants and adolescents with congenital heart disease [3,1]. Although FA measures show tissue organization and can detect pathological tissue, procedures are unable to differentiate the nature and types of injury [6], other diffusivity measures may be more sensitive to underlying pathophysiology. Diffusion tensor imaging-based MD procedures show average motion of water molecules within tissue and indicate changes in tissue microstructure. The procedures show reduced MD values in acute and increased values in chronic pathological stages and can be helpful to examine tissue injury stage in SVHD. MD values are influenced by various factors within the tissue, including tissue barriers and extracellular fluid and space, and thus, increased MD values may result from loss of cells, axonal loss, demyelination, abnormal coherence or organization of tissue [25]. In addition, AD measures show axonal integrity, and RD values correspond more closely to myelin integrity [9], and any changes in their values are believed to represent axon loss or demyelination, respectively [26]. A combination of various pathological processes underlying the disease condition may cause increased water diffusion in all directions resulting in increased MD, RD, AD, and limited FA changes and similar results have been found in early Alzheimers disease [27] and essential tremor [28]. Hence, the addition of MD, AD, RD, and FA measures provide a greater understanding of the nature and types of tissue brain injury in SVHD.

In SVHD, brain tissue changes were apparent in sites important for several cognitive functions, including memory and executive regulatory functions. These areas included the bilateral thalamus, caudate nuclei, hippocampus, para-hippocampal gyrus, fornix, mammillary bodies, corpus callosum, cerebellum, cingulate, and prefrontal cortices. The corpus callosum is a major white matter fiber bundle connecting the left and right cerebral hemispheres and transfers motor, sensory, and cognitive information between both hemispheres. The structure contains axons running to the parietal, temporal, occipital lobes, and primary and secondary somatosensory and motor areas and is involved in many cognitive functions including, attention, visuospatial processing and executive functions [29,30]. Damage to these brain areas may account for deficits in memory, motor, visuospatial processing and executive functions [31–33], which have been reported as deficient in SVHD. The limbic structures, including the hippocampus, fornix fibers, mammillary bodies, anterior thalamus, and cingulate gyrus, also showed tissue injury in SVHD. The mammillary bodies act as a hippocampal relay, passing information on to the anterior thalamus via fornix fibers and from there to the cingulate and other cortical sites, and make independent contributions to memory consolidation [34]. Damage to the hippocampus, mammillary bodies, fornix fibers, anterior thalamus, and cingulate, can result in anterograde amnesia (inability to lay down new episodic memories) [34,35]. However, damage to the parahippocampal gyrus can lead to impairment in visuospatial processing and episodic memory [36,37]. Caudate nuclei have been associated with many cognitive processes, including executive functions, and functional MRI studies have revealed co-activation of the striatum and prefrontal cortex during performances associated with executive functioning [38]. In addition, the cerebellum is involved in a variety of cognitive tasks that involve implicit and explicit learning and memory processes and working memory, along with fine motor coordination [39]. Thus, tissue changes in these brain areas may be responsible for impaired cognitive functions in SVHD.

Adolescents with SVHD show mood dysfunctions, indicating the possibility of brain injury in regions that control such functions. Increased MD values appeared in several brain sites in SVHD, including the thalamus, medial prefrontal cortices, cingulate, insular cortices, amygdala, hippocampus, and parahippocampal gyrus, responsible for regulation of mood functions. Neuroimaging, neuropathological, and lesion studies implicate that brain circuits that include the limbic-cortical-striatal-pallidal-thalamic (LCSPT) circuits, formed by connections between the orbital and medial prefrontal cortex, amygdala, hippocampus, ventromedial striatum (caudate and putamen), mediodorsal, and midline thalamic nuclei and ventral pallidum [40], regulate the evaluative, expressive, and experiential aspects of emotional behavior in mood disorders [41]. Thus, lesions within the LCSPT structures themselves or in the interconnections among them could result in depression, or anxiety as found in adolescents with SVHD.

SVHD also showed increased MD values in brain regions responsible for autonomic regulation, and including the cerebellum, hippocampus, hypothalamus, amygdala, anterior cingulate, and insula. Several studies have shown the cortical circuitry related to autonomic adjustments to many stressors in awake humans and revealed many forebrain sites that associate strongly with cardiovascular arousal during stress, including the insular cortex, anterior cingulate, amygdala, and hippocampus [42,43]. However, cerebellar and hypothalamus regions are also implicated in autonomic regulation during respiratory and cardiac challenges, as suggested by several functional MRI studies [44]. Thus, any damage to these regions may contribute to disturbances in autonomic functions [heart rate variability] in SVHD.

The cause of brain tissue injury in adolescents with SVHD is unknown, but is speculated as being multi-factorial. Delayed brain development seen in complex heart disease can make the brain tissue vulnerable to insult in SVHD [45]. In addition, other potential factors may contribute to brain injury, including hypoxia-ischemia, hypotension, and abnormal cerebral blood flow and autoregulation in the condition.

Children with SVHD show higher rates of brain abnormalities at each stage of surgery. MRI studies have been used to determine the prevalence of periventricular leukomalacia (PVL) in infants with CHD before and after surgical repair [46,47]. These studies showed occurrence of PVL 20% before and over 50% after surgery. In addition, adolescents with single ventricle, who underwent the Fontan procedure, were found to be at increased risk for psychiatric dysfunction, specifically for ADHD and anxiety disorders [48]. Surgical procedures used in these patients involve cardiopulmonary bypass, which may result in brain injury due to embolism, inflammation, and ischemia [49].

Several limitations of our study have to be mentioned, including the small sample size. Although the sample size is small, differences appeared between groups, suggesting significantly large effect sizes between SVHD and controls. Also, the SVHD group was homogeneous, and selection bias secondary to screening criteria may reflect better health within this chronic condition. Thus, our findings may not be generalizable to all SVHD participants. In addition, it is difficult to separate the effects of operative, developmental, or physiologic factors that may have contributed to brain injury.

CONCLUSIONS

Adolescents with SVHD, over a decade from their last surgical procedure, showed widespread brain abnormalities in autonomic, mood, and cognitive regulatory areas, and these brain injuries were predominantly due to myelin changes. These sites included the insular cortices, caudate nuclei, cingulate, hypothalamus, mid-corona radiata, thalamus, medial prefrontal and prefrontal cortices, parahippocampal gyrus, hippocampus, precentral gyrus, amygdala, cerebellar cortices, corpus callosum, basal forebrain, mammillary bodies, internal capsule, midbrain, fornix, occipital, parietal, frontal and temporal cortices. These findings indicate that brain injury is in the chronic pathological stage in SVHD patients with predominant myelin changes, which may result from hypoxia/ischemia- or developmental-induced changes in the condition.

Acknowledgements:

Authors would like to thank Patty Chung, and Paola Moreno for assistance with data collection.

Funding: This study was funded by the National Institutes of Health R01NR016463.

References

1. Mulkey SB, Ou X, Ramakrishnaiah RH, Glasier CM, Swearingen CJ, Melguizo MS, Yap VL, Schmitz ML, Bhutta AT (2014) White matter injury in newborns with congenital heart disease: a diffusion tensor imaging study. Pediatric neurology 51 (3):377–383 [PubMed: 25160542]
2. Rollins CK, Watson CG, Asaro LA, Wypij D, Vajapeyam S, Bellinger DC, DeMaso DR, Robertson RL Jr., Newburger JW, Rivkin MJ (2014) White matter microstructure and cognition in adolescents with congenital heart disease. J Pediatr 165 (5):936–944 e931–932 [PubMed: 25217200]
3. Rivkin MJ, Watson CG, Scoppettuolo LA, Wypij D, Vajapeyam S, Bellinger DC, DeMaso DR, Robertson RL, Newburger JW (2013) Adolescents with D-transposition of the great arteries repaired in early infancy demonstrate reduced white matter microstructure associated with clinical risk factors. J Thorac Cardiov Sur 146 (3):543–U593
4. Nath K, Saraswat VA, Krishna YR, Thomas MA, Rathore RKS, Pandey CM, Gupta RK (2008) Quantification of cerebral edema on diffusion tensor imaging in acute-on-chronic liver failure. Nmr in Biomedicine 21 (7):713–722 [PubMed: 18384180]
5. Newcombe V, Chatfield D, Outtrim J, Vowler S, Manktelow A, Cross J, Scoffings D, Coleman M, Hutchinson P, Coles J, Carpenter TA, Pickard J, Williams G, Menon D (2011) Mapping traumatic axonal injury using diffusion tensor imaging: correlations with functional outcome. PloS one 6 (5):e19214 [PubMed: 21573228]
6. Basser PJ, Pierpaoli C (1996) Microstructural and physiological features of tissues elucidated by quantitative-diffusion-tensor MRI. J Magn Reson Ser B 111 (3):209–219 [PubMed: 8661285]
7. Woo MA, Palomares JA, Macey PM, Fonarow GC, Harper RM, Kumar R (2015) Global and regional brain mean diffusivity changes in patients with heart failure. J Neurosci Res 93 (4):678–685 [PubMed: 25502071]
8. Kumar R, Chavez AS, Macey PM, Woo MA, Yan-Go FL, Harper RM (2012) Altered global and regional brain mean diffusivity in patients with obstructive sleep apnea. J Neurosci Res 90 (10): 2043–2052 [PubMed: 22715089]
9. Song SK, Sun SW, Ju WK, Lin SJ, Cross AH, Neufeld AH (2003) Diffusion tensor imaging detects and differentiates axon and myelin degeneration in mouse optic nerve after retinal ischemia. NeuroImage 20 (3):1714–1722 [PubMed: 14642481]
10. Ontaneda D, Sakaie K, Lin J, Wang XF, Lowe MJ, Phillips MD, Fox RJ (2017) Measuring Brain Tissue Integrity during 4 Years Using Diffusion Tensor Imaging. AJNR American journal of neuroradiology 38 (1):31–38 [PubMed: 27659189]
11. Stebbins GT, Murphy CM (2009) Diffusion tensor imaging in Alzheimer's disease and mild cognitive impairment. Behavioural neurology 21 (1):39–49 [PubMed: 19847044]
12. Hashim E, Caverzasi E, Papinutto N, Lewis CE, Jing RW, Charles O, Zhang SD, Lin A, Graham SJ, Schweizer TA, Bharatha A, Cusimano MD (2017) Investigating Microstructural Abnormalities and Neurocognition in Sub-Acute and Chronic Traumatic Brain Injury Patients with Normal-Appearing White Matter: A Preliminary Diffusion Tensor Imaging Study. Front Neurol 8
13. Kumar R, Pham TT, Macey PM, Woo MA, Yan-Go FL, Harper RM (2014) Abnormal myelin and axonal integrity in recently diagnosed patients with obstructive sleep apnea. Sleep 37 (4):723–732 [PubMed: 24899761]

14. Kumar R, Woo MA, Macey PM, Fonarow GC, Hamilton MA, Harper RM (2011) Brain axonal and myelin evaluation in heart failure. J Neurol Sci 307 (1–2):106–113 [PubMed: 21612797]
15. Kumar R, Macey PM, Woo MA, Harper RM (2010) Rostral brain axonal injury in congenital central hypoventilation syndrome. J Neurosci Res 88 (10):2146–2154 [PubMed: 20209631]
16. Beck AT, Epstein N, Brown G, Steer RA (1988) An inventory for measuring clinical anxiety: psychometric properties. J Consult Clin Psychol 56 (6):893–897 [PubMed: 3204199]
17. Kroenke K, Spitzer RL, Williams JB (2001) The PHQ-9: validity of a brief depression severity measure. Journal of general internal medicine 16 (9):606–613 [PubMed: 11556941]
18. Nasreddine ZS, Phillips NA, Bedirian V, Charbonneau S, Whitehead V, Collin I, Cummings JL, Chertkow H (2005) The Montreal Cognitive Assessment, MoCA: a brief screening tool for mild cognitive impairment. J Am Geriatr Soc 53 (4):695–699 [PubMed: 15817019]
19. Pike NA, Poulsen MK, Woo MA (2017) Validity of the Montreal Cognitive Assessment Screener in Adolescents and Young Adults With and Without Congenital Heart Disease. Nursing research 66 (3):222–230 [PubMed: 28448372]
20. Sheslow D, Adams W (2003) Wide range assessment of memory and learning administration and technical manual (2nd ed.). Wide Range Inc, Wilmington, DE
21. Zhang H, Yushkevich PA, Alexander DC, Gee JC (2006) Deformable registration of diffusion tensor MR images with explicit orientation optimization. Med Image Anal 10 (5):764–785 [PubMed: 16899392]
22. Le Bihan D, Mangin JF, Poupon C, Clark CA, Pappata S, Molko N, Chabriat H (2001) Diffusion tensor imaging: Concepts and applications. J Magn Reson Imaging 13 (4):534–546. doi:DOI 10.1002/jmri.1076 [PubMed: 11276097]
23. Ashburner J, Friston KJ (2005) Unified segmentation. NeuroImage 26 (3):839–851 [PubMed: 15955494]
24. von Rhein M, Scheer I, Loenneker T, Huber R, Knirsch W, Latal B (2011) Structural brain lesions in adolescents with congenital heart disease. J Pediatr 158 (6):984–989 [PubMed: 21237469]
25. Lebihan D, Moonen CTW, Vanzijl PCM, Pekar J, Despres D (1991) Measuring Random Microscopic Motion of Water in Tissues with Mr Imaging - a Cat Brain Study. J Comput Assist Tomo 15 (1):19–25
26. Wheeler-Kingshott CA, Cercignani M (2009) About “axial” and “radial” diffusivities. Magnetic resonance in medicine 61 (5):1255–1260 [PubMed: 19253405]
27. Acosta-Cabronero J, Williams GB, Pengas G, Nestor PJ (2010) Absolute diffusivities define the landscape of white matter degeneration in Alzheimer’s disease. Brain 133 (Pt 2):529–539 [PubMed: 19914928]
28. Saini J, Bagepally BS, Bhatt MD, Chandran V, Bharath RD, Prasad C, Yadav R, Pal PK (2012) Diffusion tensor imaging: tract based spatial statistics study in essential tremor. Parkinsonism Relat Disord 18 (5):477–482 [PubMed: 22297126]
29. Gooijers J, Swinnen SP (2014) Interactions between brain structure and behavior: The corpus callosum and bimanual coordination. Neurosci Biobehav R 43:1–19
30. Aralasmak A, Ulmer JL, Kocak M, Salvan CV, Hillis AE, Yousem DM (2006) Association, commissural, and projection pathways and their functional deficit reported in literature. J Comput Assist Tomo 30 (5):695–715
31. Pike NA, Woo MA, Poulsen MK, Evangelista W, Faire D, Halnon NJ, Lewis AB, Kumar R (2016) Predictors of Memory Deficits in Adolescents and Young Adults with Congenital Heart Disease Compared to Healthy Controls. Frontiers in pediatrics 4:117 [PubMed: 27843890]
32. Cassidy AR, White MT, DeMaso DR, Newburger JW, Bellinger DC (2015) Executive Function in Children and Adolescents with Critical Cyanotic Congenital Heart Disease. Journal of the International Neuropsychological Society : JINS 21 (1):34–49 [PubMed: 25487044]
33. Liamlahi R, von Rhein M, Buhrer S, Valsangiacomo Buechel ER, Knirsch W, Landolt MA, Latal B (2014) Motor dysfunction and behavioural problems frequently coexist with congenital heart disease in school- age children. Acta paediatrica 103 (7):752–758 [PubMed: 24661017]
34. Vann SD, Nelson AJD (2015) The mammillary bodies and memory: more than a hippocampal relay. Prog Brain Res 219:163–185 [PubMed: 26072239]

35. Clarke S, Assal G, Bogousslavsky J, Regli F, Townsend DW, Leenders KL, Blecic S (1994) Pure Amnesia after Unilateral Left Polar Thalamic Infarct - Topographic and Sequential Neuropsychological and Metabolic (Pet) Correlations. J Neurol Neurosur Ps 57 (1):27–34
36. Aminoff EM, Kveraga K, Bar M (2013) The role of the parahippocampal cortex in cognition. Trends in cognitive sciences 17 (8):379–390 [PubMed: 23850264]
37. Ploner CJ, Gaymard BM, Rivaud-Pechoux S, Baulac M, Clemenceau S, Samson S, Pierrot-Deseilligny C (2000) Lesions affecting the parahippocampal cortex yield spatial memory deficits in humans. Cereb Cortex 10 (12):1211–1216 [PubMed: 11073870]
38. Hedden T, Gabrieli JD (2010) Shared and selective neural correlates of inhibition, facilitation, and shifting processes during executive control. NeuroImage 51 (1):421–431 [PubMed: 20123030]
39. Desmond JE, Fiez JA (1998) Neuroimaging studies of the cerebellum: language, learning and memory. Trends in cognitive sciences 2 (9):355–362 [PubMed: 21227232]
40. Drevets WC, Price JL, Furey ML (2008) Brain structural and functional abnormalities in mood disorders: implications for neurocircuitry models of depression. Brain Struct Funct 213 (1–2):93–118 [PubMed: 18704495]
41. Phillips ML, Drevets WC, Rauch SL, Lane R (2003) Neurobiology of emotion perception II: Implications for major psychiatric disorders. Biol Psychiat 54 (5):515–528 [PubMed: 12946880]
42. Shoemaker JK, Goswami R (2015) Forebrain neurocircuitry associated with human reflex cardiovascular control. Front Physiol 6
43. Harper RM, Bandler R, Spriggs D, Alger JR (2000) Lateralized and widespread brain activation during transient blood pressure elevation revealed by magnetic resonance imaging. J Comp Neurol 417 (2):195–204 [PubMed: 10660897]
44. Harper RM, Gozal D, Bandler R, Spriggs D, Lee J, Alger J (1998) Regional brain activation in humans during respiratory and blood pressure challenges. Clinical and experimental pharmacology & physiology 25 (6):483–486 [PubMed: 9673830]
45. Sethi V, Tabbutt S, Dimitropoulos A, Harris KC, Chau V, Poskitt K, Campbell A, Azakie A, Xu D, Barkovich AJ, Miller SP, McQuillen PS (2013) Single-ventricle anatomy predicts delayed microstructural brain development. Pediatric research 73 (5):661–667 [PubMed: 23407116]
46. Mahle WT, Tavani F, Zimmerman RA, Nicolson SC, Galli KK, Gaynor JW, Clancy RR, Montenegro LM, Spray TL, Chiavacci RM, Wernovsky G, Kurth CD (2002) An MRI study of neurological injury before and after congenital heart surgery. Circulation 106 (12 Suppl 1):I109–114 [PubMed: 12354718]
47. Mebius MJ, Kooi EMW, Bilardo CM, Bos AF (2017) Brain Injury and Neurodevelopmental Outcome in Congenital Heart Disease: A Systematic Review. Pediatrics 140 (1)
48. DeMaso DR, Calderon J, Taylor GA, Holland JE, Stopp C, White MT, Bellinger DC, Rivkin MJ, Wypij D, Newburger JW (2017) Psychiatric Disorders in Adolescents With Single Ventricle Congenital Heart Disease. Pediatrics 139 (3)
49. Miller SP, McQuillen PS, Hamrick S, Xu D, Glidden DV, Charlton N, Karl T, Azakie A, Ferriero DM, Barkovich AJ, Vigneron DB (2007) Abnormal brain development in newborns with congenital heart disease. N Engl J Med 357 (19):1928–1938 [PubMed: 17989385]

Author Manuscript
Author Manuscript
Author Manuscript

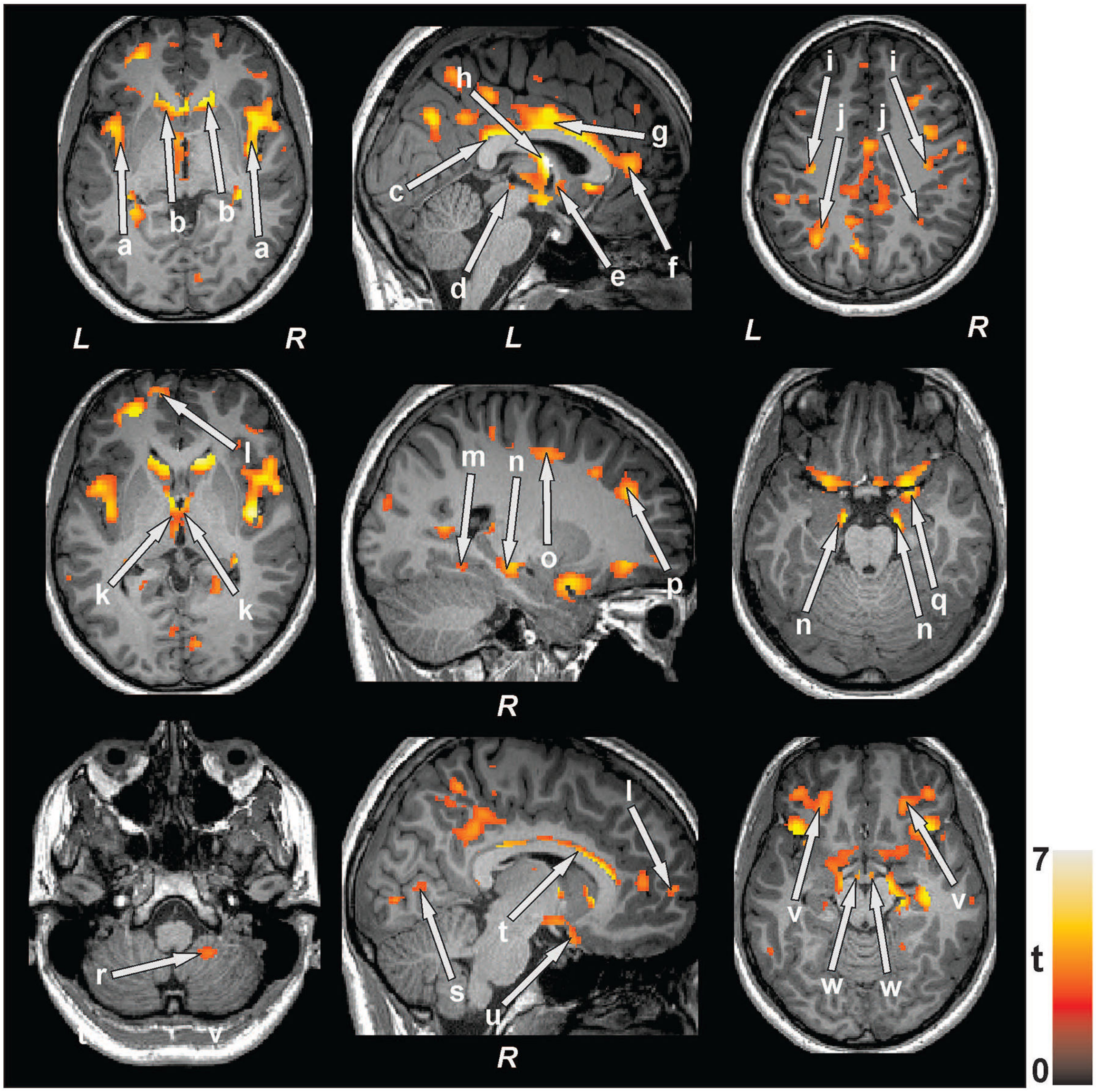

Fig. 1:

Brain sites with increased mean diffusivity (MD) values in SVHD compared to control subjects. Brain regions showed increased MD values in the bilateral insular cortices (a), bilateral caudate nuclei (b), anterior (f), mid (g), and posterior (c) cingulate cortices, midbrain (d), hypothalamus (e), fornix (h), bilateral mid-corona radiata (i), bilateral parietal cortices (j), bilateral thalamus (k), bilateral medial prefrontal cortices (l), para-hippocampal gyrus (m), bilateral hippocampus (n), precentral gyrus (o), frontal gyrus (p), amygdala (q), cerebellar cortices (r), bilateral occipital cortices (s), corpus callosum (t), basal forebrain (u), bilateral prefrontal cortices (v), and bilateral mammillary bodies (w), in SVHD over controls. All images are in neurological convention (*L = Left; R = Right*). Color bar indicates t-statistic values.

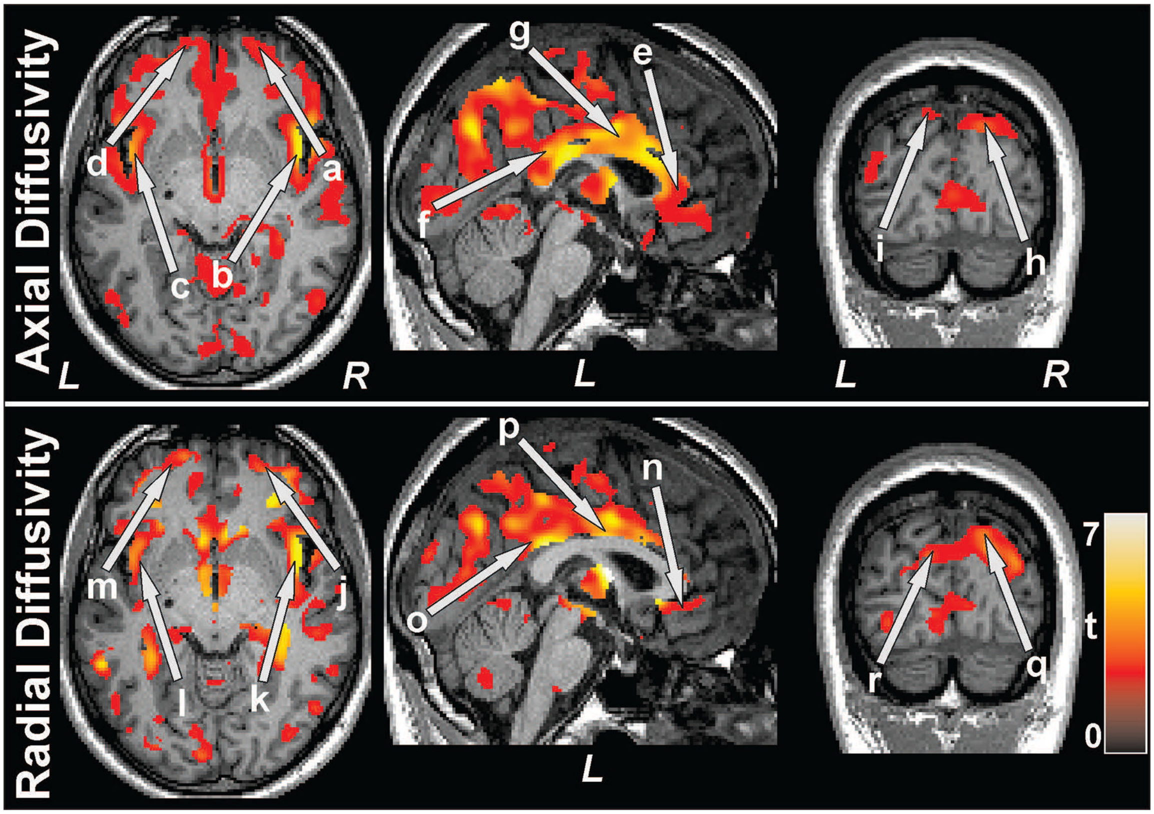

Fig. 2:

Brain regions with increased axial diffusivity and radial diffusivity values in SVHD over control subjects. These sites included the bilateral prefrontal cortices (a, d, j, m), bilateral insula (b, c, k, l), left anterior (e, n), mid (g, p) and posterior (f, o) cingulate, and bilateral occipital cortex (h, i, q, r). Figure conventions are same as in Figure 1.

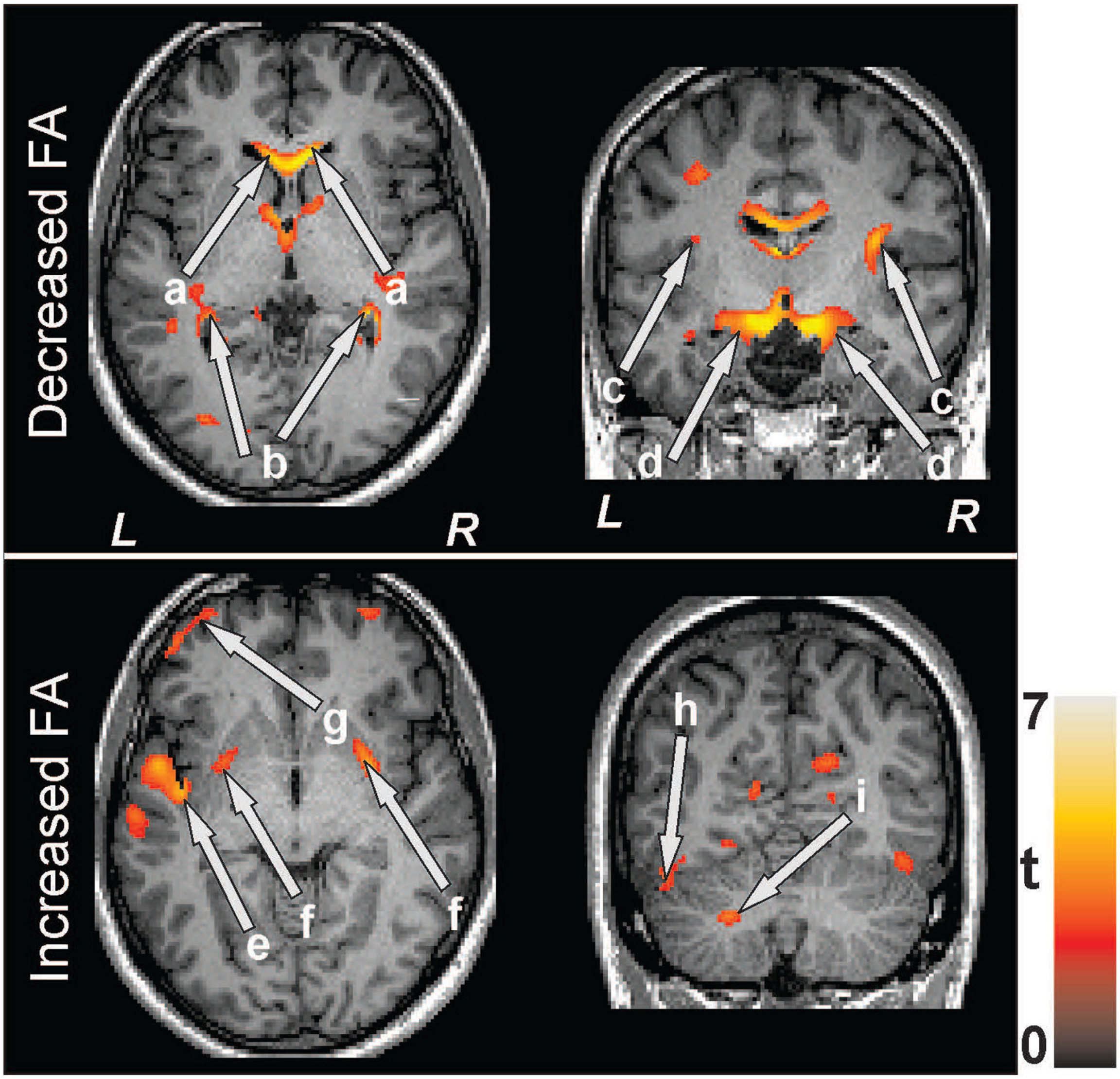

Fig. 3:
Brain areas with decreased or increased FA values in SVHD over controls. Lower FA values emerged in the bilateral corpus callosum (a), hippocampus (b), anterior insula (c), and amygdala (d), and higher FA values appeared in the posterior insula (e), putamen (f), prefrontal cortices (g), cerebellar cortices (h), and posterior cerebellar peduncle (i) in SVHD over controls. Figure conventions are same as in Figure 1.

Author Manuscript

Author Manuscript

Author Manuscript

Table 1.

Demographic, mood, cognitive, and clinical characteristics of SVHD and controls.

Variables	SVHD n = 27 (Mean ± SD)	Controls n = 35 (Mean ± SD)	P values
Age (years)	15.7±1.2	15.9±1.2	0.44
Gender [male] (%)	15 (56%)	18 (51%)	0.75
Ethnicity (%)			0.74
White	12 (44%)	19 (55%)	
Hispanic	12 (44%)	13 (37%)	
Other	3 (11%)	3 (8%)	
BMI (kg/m^2)	22.8±5.6	22.2±4.0	0.62
Handedness [right] (%)	23 (85%)	32 (91%)	0.45
Single Ventricle Diagnosis (%):		N/A	N/A
DORV/Unbalanced AVC/HLV	7 (26%)		
HLHS	6 (22%)		
Unbalanced AVC/HRV	5 (19%)		
Tricuspid Atresia	4 (15%)		
Pulmonary Atresia/IVS/HRV	3 (11%)		
DILV	2 (7%)		
Ventricle type [right] (%)	16 (67%)	N/A	N/A
Extracardiac Fontan (%)	21 (78%)	N/A	N/A
Fenestration (%)	7 (26%)	N/A	N/A
*Residual Cyanosis (%)	7 (26%)	N/A	N/A
Number of Surgeries	3.0 ± 0.6	N/A	N/A
# Years Since Last Surgery	12.6 ± 3.9 (n=24)	N/A	N/A
PHQ-9	6.7±5.2	3.7±2.7	0.005
BAI	19.9±14.3	9.0±7.7	<0.001
WRAML2 GMI	84.0±12.0	108.7±12.5	<0.001
WRAML2: Verbal Memory	88.3±12.6	106.5±11.3	<0.001
WRAML2: Visual Memory	99.7±12.7	108.0±11.8	0.01
WRAML2: Attention	84.6±10.1	107.7±7.7	<0.001
WRAML2 GRI	90.4±10.6 (n=26)	111.3±11.5 (n=34)	<0.001
WRAML2: Working Recognition	87.0±12.5	107.3±19.1	<0.001
WRAML2: Verbal Recognition	91.5±11.4	103.3±18.8 (n=34)	0.006
WRAML2: Visual Recognition	93.4±12.8 (n=26)	104.1±17.7	0.007
Total MoCA scores	21.7±4.1	28.8±1.7	<0.001
MoCA: Visuospatial	3.3±1.4	4.9±0.4	<0.001
MoCA: Naming	2.9±0.3	3.0±0.0	0.04
MoCA: Attention	3.9±1.5	5.7±0.7	<0.001
MoCA: Language	1.6± 1. 0	2.6±0.6	<0.001

Author Manuscript
Author Manuscript
Author Manuscript

Variables	SVHD n = 27 (Mean ± SD)	Controls n = 35 (Mean ± SD)	P values
MoCA: Abstraction	1.2±0.7	1.9±0.4	<0.001
MoCA: Delayed Recall	2.1±1.5	4.1±1.0	<0.001
MoCA: Orientation	5.7±0.7	5.9±0.4	0.21

SD = Standard Deviation; N/A = Not Applicable; BMI = Body Mass Index; HLHS= Hypoplastic Left Heart Syndrome; DORV = Double Outlet Right Ventricle; DILV= Double Inlet Left Ventricle; IVS= Intact Ventricular Septum; HLV = Hypoplastic Left Ventricle; HRV= Hypoplastic Right Ventricle; AVC = Atrioventricular Canal Defect; PHQ-9= Patient Health Questionnaire-9; BAI= Beck Anxiety Inventory; WRAML2 = Wide Range Assessment of Memory and Learning, 2nd Edition; GMI = General Memory Index; GRI = General Memory Recognition Index; MoCA= Montreal Cognitive Assessment;

*Pulse Oximetry < 93%.

Table 2.

Clinical imaging characteristics of SVHD subjects.

Subject ID	Brain Abnormalities
1	A 7×10 cystic focus in right pterygoid space
2	Normal
3	Normal
4	Normal
5	Periventricular white matter change, most likely gliosis or chronic insult
6	Pituitary gland is abnormal with Rathke's cleft cust and possible adenoma
7	Normal
8	Old tissue loss with encephalomalacia of the right inferior cerebellum. Calcification or sequela of micro hemorrhage in right frontal operculum
9	Normal
10	Normal
11	Normal
12	Old left MCA territory infarction with encephalomalacia of the left inferior frontal gyrus
13	Old ischemic changes in the periventricular white matter. Small lacunar infarct in the right thalamus
14	Normal
15	Normal
16	Normal
17	Normal
18	N/A
19	Normal
20	Normal
21	Normal
22	Chronic ischemic change is seen in periventricular white matter
23	Chiari I malformation
24	Old infarctions of the bilateral posterior cerbral artery territories including right medial temporal and occipital lobes and left superior parietal lobe
25	Old infarct of the right putamen. No new infarction or white matter changes
26	Normal
27	Rathke's cleft cyst

Table 3:

Regional brain mean diffusivity ($\times10^{-3}$ mm^2/s) differences between SVHD and control subjects corrected for age and sex.

Brain region	SVHD (mean ± SD) n = 27	Control (mean ± SD) n = 35	P value	Effect Size
R Thalamus	1.36 ± 0.12	1.18 ± 0.12	< 0.001	1.50
L Thalamus	1.38 ± 0.13	1.18 ± 0.13	< 0.001	1.54
R Hippocampus	1.25 ± 0.14	1.10 ± 0.14	< 0.001	1.07
L Hippocampus	1.27 ± 0.07	1.15 ± 0.07	< 0.001	1.71
R Parahippocampal Gyrus	1.49 ± 0.13	1.33 ± 0.13	< 0.001	1.23
L Parahippocampal Gyrus	1.36 ± 0.09	1.26 ± 0.09	< 0.001	1.11
R Hypothalamus	1.59 ± 0.18	1.40 ± 0.18	< 0.001	1.05
L Hypothalamus	1.20 ± 0.14	1.05 ± 0.14	< 0.001	1.07
R Mammillary Bodies	1.48 ± 0.16	1.28 ± 0.16	< 0.001	1.25
L Mammillary Bodies	1.49 ± 0.17	1.29 ± 0.17	< 0.001	1.18
R Amygdala	1.24 ± 0.10	1.13 ± 0.10	< 0.001	1.10
L Amygdala	1.23 ± 0.10	1.11 ± 0.10	< 0.001	1.20
R Caudate Nucleus	1.27 ± 0.15	1.06 ± 0.15	< 0.001	1.40
L Caudate Nucleus	1.20 ± 0.14	1.00 ± 0.14	< 0.001	1.43
R Mid Corona-radiata	0.83 ± 0.04	0.78 ± 0.04	< 0.001	1.25
L Mid Corona-radiata	0.82 ± 0.03	0.78 ± 0.03	< 0.001	1.33
R Internal Capsule	0.78 ± 0.04	0.74 ± 0.04	< 0.001	1.00
L Internal Capsule	0.84 ± 0.05	0.79 ± 0.05	< 0.001	1.00
Fornix	1.69 ± 0.17	1.39 ± 0.17	< 0.001	1.77
R Midbrain	1.12 ± 0.10	1.01 ± 0.10	< 0.001	1.10
L Midbrain	1.17 ± 0.10	1.05 ± 0.10	< 0.001	1.20
R Insula	1.17 ± 0.09	1.04 ± 0.09	< 0.001	1.44
L Insula	1.15 ± 0.07	1.02 ± 0.07	< 0.001	1.86
R Anterior Cingulate	1.05 ± 0.09	0.94 ± 0.09	< 0.001	1.22
L Anterior Cingulate	1.04 ± 0.09	0.94 ± 0.09	< 0.001	1.11
R Mid Cingulate	1.04 ± 0.08	0.94 ± 0.08	< 0.001	1.25
L Mid Cingulate	1.04 ± 0.08	0.95 ± 0.08	< 0.001	1.12
R Posterior Cingulate	1.06 ± 0.08	0.96 ± 0.08	< 0.001	1.25
L Posterior Cingulate	1.04 ± 0.07	0.94 ± 0.07	< 0.001	1.43
R Corpus Callosum	1.04 ± 0.08	0.92 ± 0.08	< 0.001	1.50
L Corpus Callosum	1.08 ± 0.09	0.96 ± 0.09	< 0.001	1.33
R Temporal Cortices	0.89 ± 0.05	0.84 ± 0.05	< 0.001	1.00
L Temporal Cortices	1.01 ± 0.07	0.92 ± 0.07	< 0.001	1.29
R Prefrontal Cortices	1.00 ± 0.06	0.91 ± 0.06	< 0.001	1.50
L Prefrontal Cortices	1.17 ± 0.11	1.06 ± 0.11	< 0.001	1.00
R Frontal Cortices	0.95 ± 0.06	0.87 ± 0.06	< 0.001	1.33

Brain region	SVHD (mean ± SD) n = 27	Control (mean ± SD) n = 35	P value	Effect Size
L Frontal Cortices	0.91 ± 0.07	0.83 ± 0.07	< 0.001	1.14
R Precentral Gyrus	0.86 ± 0.05	0.80 ± 0.05	< 0.001	1.20
L Precentral Gyrus	0.95 ± 0.06	0.87 ± 0.06	< 0.001	1.33
R Basal Forebrain	1.12 ± 0.11	1.01 ± 0.11	< 0.001	1.00
L Basal Forebrain	1.14 ± 0.11	1.02 ± 0.11	< 0.001	1.09
R Occipital Cortices	0.90 ± 0.06	0.85 ± 0.06	0.005	0.83
L Occipital Cortices	0.91 ± 0.06	0.85 ± 0.06	< 0.001	1.00
R Parietal Cortices	0.93 ± 0.07	0.86 ± 0.07	< 0.001	1.00
L Parietal Cortices	0.97 ± 0.09	0.87 ± 0.09	0.002	1.11
R Cerebellar Cortices	1.16 ± 0.10	1.06 ± 0.10	< 0.001	1.00
L Cerebellar Cortices	0.77 ± 0.07	0.70 ± 0.07	0.001	1.00

SVHD, Single Ventricle Heart Disease; L, Left; R, Right.

Table 4:

Regional brain axial diffusivity ($\times 10^{-3}$ mm^2/s) differences between SVHD and control subjects corrected for age and sex.

Brain region	SVHD (mean ± SD) n = 27	Control (mean ± SD) n = 35	P value	Effect Size
R Thalamus	1.68 ± 0.20	1.46 ± 0.20	< 0.001	1.10
L Thalamus	1.57 ± 0.20	1.38 ± 0.20	0.001	0.95
R Hippocampus	1.84 ± 0.28	1.56 ± 0.28	< 0.001	1.00
R Parahippocampal Gyrus	1.37 ± 0.19	1.26 ± 0.19	0.017	0.58
R Hypothalamus	1.45 ± 0.20	1.27 ± 0.20	0.001	0.90
L Hypothalamus	1.81 ± 0.25	1.58 ± 0.25	0.001	0.92
R Mammillary Bodies	1.84 ± 0.26	1.6 ± 0.26	0.001	0.92
L Mammillary Bodies	1.81 ± 0.25	1.57 ± 0.25	< 0.001	0.96
R Amygdala	1.57 ± 0.22	1.42 ± 0.22	0.007	0.68
R Caudate Nucleus	1.53 ± 0.19	1.28 ± 0.19	< 0.001	1.32
L Caudate Nucleus	1.61 ± 0.21	1.34 ± 0.21	< 0.001	1.29
R Mid Corona-radiata	1.18 ± 0.05	1.12 ± 0.05	< 0.001	1.20
L Mid Corona-radiata	1.09 ± 0.03	1.05 ± 0.03	< 0.001	1.33
Fornix	2.10 ± 0.27	1.78 ± 0.27	< 0.001	1.19
R Midbrain	1.59 ± 0.22	1.41 ± 0.22	0.002	0.82
L Midbrain	1.50 ± 0.21	1.32 ± 0.21	0.002	0.86
R Insula	1.4 ± 0.13	1.22 ± 0.13	< 0.001	1.39
L Insula	1.32 ± 0.13	1.18 ± 0.13	< 0.001	1.08
R Anterior Cingulate	1.46 ± 0.13	1.32 ± 0.13	< 0.001	1.08
L Anterior Cingulate	1.45 ± 0.13	1.3 ± 0.13	< 0.001	1.15
R Mid Cingulate	1.4 ± 0.10	1.28 ± 0.10	< 0.001	1.70
L Mid Cingulate	1.36 ± 0.09	1.24 ± 0.09	< 0.001	1.33
R Posterior Cingulate	1.4 ± 0.08	1.31 ± 0.08	< 0.001	1.13
L Posterior Cingulate	1.24 ± 0.07	1.17 ± 0.07	0.001	1.00
R Corpus Callosum	1.58 ± 0.20	1.41 ± 0.20	0.001	0.85
L Corpus Callosum	1.61 ± 0.19	1.44 ± 0.19	0.001	0.90
R Temporal Cortices	1.19 ± 0.13	1.06 ± 0.13	<0.001	1.00
R Prefrontal Cortices	1.34 ± 0.10	1.22 ± 0.10	< 0.001	1.20
L Prefrontal Cortices	1.4 ± 0.16	1.23 ± 0.15	< 0.001	1.10
R Frontal Cortices	1.21 ± 0.06	1.13 ± 0.06	< 0.001	1.33
L Frontal Cortices	1.2 ± 0.06	1.1 ± 0.06	< 0.001	1.67
R Precentral Gyrus	1.37 ± 0.13	1.24 ± 0.13	< 0.001	1.00
L Precentral Gyrus	1.25 ± 0.10	1.15 ± 0.10	< 0.001	1.00
R Basal Forebrain	1.42 ± 0.20	1.25 ± 0.20	0.001	0.90
L Basal Forebrain	1.39 ± 0.20	1.23 ± 0.20	0.002	0.80
R Occipital Cortices	1.21 ± 0.16	1.08 ± 0.15	0.002	0.84

Brain region	SVHD (mean ± SD) n = 27	Control (mean ± SD) n = 35	P value	Effect Size
R Parietal Cortices	1.18 ± 0.10	1.05 ± 0.10	< 0.001	1.3
L Parietal Cortices	1.21 ± 0.10	1.11 ± 0.10	0.001	1.00
R Cerebellar Cortices	1.67 ± 0.16	1.51 ± 0.16	< 0.001	0.99
L Cerebellar Cortices	1.55 ± 0.15	1.40 ± 0.15	< 0.001	1.00

SVHD, Single Ventricle Heart Disease; L, Left; R, Right.

Table 5:

Regional brain radial diffusivity ($\times 10^{-3}$ mm^2/s) differences between SVHD and control subjects corrected for age and sex.

Brain region	SVHD (mean ± SD) n = 27	Control (mean ± SD) n = 35	P value	Effect Size
R Thalamus	1.20 ± 0.13	1.00 ± 0.13	< 0.001	1.54
L Thalamus	1.18 ± 0.12	1.00 ± 0.12	< 0.001	1.50
R Hippocampus	1.03 ± 0.08	0.90 ± 0.08	< 0.001	1.63
L Hippocampus	1.08 ± 0.14	0.93 ± 0.14	< 0.001	1.07
R Parahippocampal Gyrus	0.82 ± 0.06	0.77 ± 0.06	0.005	0.83
L Parahippocampal Gyrus	0.90 ± 0.06	0.86 ± 0.06	0.015	0.67
R Hypothalamus	1.36 ± 0.18	1.21 ± 0.18	0.002	0.83
L Hypothalamus	0.99 ± 0.09	0.90 ± 0.09	< 0.001	1.00
R Mammillary Bodies	1.37 ± 0.18	1.16 ± 0.18	< 0.001	1.17
L Mammillary Bodies	1.36 ± 0.17	1.14 ± 0.17	< 0.001	1.29
R Amygdala	1.01 ± 0.08	0.91 ± 0.08	< 0.001	1.25
L Amygdala	1.01 ± 0.08	0.93 ± 0.08	< 0.001	1.00
R Caudate Nucleus	1.05 ± 0.14	0.86 ± 0.14	< 0.001	1.36
L Caudate Nucleus	1.13 ± 0.15	0.92 ± 0.15	< 0.001	1.40
R Mid Corona-radiata	0.63 ± 0.03	0.59 ± 0.03	< 0.001	1.33
L Mid Corona-radiata	0.65 ± 0.05	0.61 ± 0.05	0.001	0.80
R Internal Capsule	0.65 ± 0.03	0.61 ± 0.03	< 0.001	1.33
L Internal Capsule	0.68 ± 0.04	0.64 ± 0.04	< 0.001	1.00
Fornix	1.43 ± 0.16	1.14 ± 0.16	< 0.001	1.81
R Midbrain	1.04 ± 0.09	0.93 ± 0.09	< 0.001	1.22
L Midbrain	0.99 ± 0.09	0.87 ± 0.09	< 0.001	1.33
R Insula	1.10 ± 0.07	0.97 ± 0.07	< 0.001	1.86
L Insula	1.00 ± 0.08	0.91 ± 0.08	< 0.001	1.12
R Anterior Cingulate	0.84 ± 0.09	0.74 ± 0.09	< 0.001	1.11
L Anterior Cingulate	0.90 ± 0.08	0.79 ± 0.08	< 0.001	1.37
R Mid Cingulate	0.87 ± 0.08	0.78 ± 0.08	< 0.001	1.12
L Mid Cingulate	0.85 ± 0.07	0.77 ± 0.07	< 0.001	1.14
R Posterior Cingulate	0.87 ± 0.08	0.76 ± 0.08	< 0.001	1.37
L Posterior Cingulate	0.84 ± 0.06	0.76 ± 0.06	< 0.001	1.33
R Corpus Callosum	0.84 ± 0.10	0.69 ± 0.10	< 0.001	1.50
L Corpus Callosum	0.97 ± 0.11	0.79 ± 0.11	< 0.001	1.64
R Temporal Cortices	0.78 ± 0.04	0.73 ± 0.04	< 0.001	1.25
L Temporal Cortices	1.09 ± 0.13	0.98 ± 0.13	0.002	0.85
R Prefrontal Cortices	1.06 ± 0.12	0.95 ± 0.12	0.001	0.92
L Prefrontal Cortices	0.92 ± 0.08	0.82 ± 0.08	< 0.001	1.25
R Frontal Cortices	0.91 ± 0.07	0.82 ± 0.07	< 0.001	1.29

Brain region	SVHD (mean ± SD) n = 27	Control (mean ± SD) n = 35	P value	Effect Size
L Frontal Cortices	0.80 ± 0.06	0.73 ± 0.06	< 0.001	1.17
R Precentral Gyrus	0.92 ± 0.07	0.84 ± 0.07	< 0.001	1.14
L Precentral Gyrus	0.73 ± 0.06	0.67 ± 0.06	< 0.001	1.00
R Basal Forebrain	0.97 ± 0.11	0.87 ± 0.11	< 0.001	0.91
L Basal Forebrain	1.01 ± 0.11	0.90 ± 0.11	< 0.001	1.00
R Occipital Cortices	0.83 ± 0.08	0.76 ± 0.08	< 0.001	0.87
L Occipital Cortices	0.78 ± 0.05	0.71 ± 0.05	< 0.001	1.40
R Parietal Cortices	0.88 ± 0.08	0.81 ± 0.08	0.001	0.87
L Parietal Cortices	0.83 ± 0.08	0.76 ± 0.08	< 0.001	0.87
R Cerebellar Cortices	0.96 ± 0.09	0.86 ± 0.09	< 0.001	1.11
L Cerebellar Cortices	1.16 ± 0.12	1.04 ± 0.12	< 0.001	1.00

SVHD, Single Ventricle Heart Disease; L, Left; R, Right.

Table 6:

Regional brain fractional anisotropy (FA) differences between SVHD and control subjects corrected for age and sex.

Brain region	SVHD (mean ± SD) n = 27	Control (mean ± SD) n = 35	P value	Effect Size
Brain regions with decreased FA in SVHD				
L Anterior Insula	0.29 ± 0.02	0.30 ± 0.02	0.001	0.50
R Anterior Insula	0.29 ± 0.02	0.31 ± 0.02	0.002	1.00
L Amygdala	0.29 ± 0.03	0.32 ± 0.03	<0.001	1.00
R Amygdala	0.29 ± 0.03	0.33 ± 0.03	<0.001	1.33
L Caudate	0.21 ± 0.03	0.24 ± 0.03	<0.001	1.00
R Caudate	0.23 ± 0.03	0.26 ± 0.03	<0.001	1.00
L Hippocampus	0.32 ± 0.03	0.35 ± 0.03	<0.001	1.00
R Hippocampus	0.29 ± 0.03	0.33 ± 0.03	<0.001	1.33
L Thalamus	0.29 ± 0.02	0.32 ± 0.02	<0.001	1.50
R Thalamus	0.29 ± 0.02	0.32 ± 0.02	<0.001	1.50
L Corpus Callosum	0.50 ± 0.04	0.55 ± 0.04	<0.001	1.25
R Corpus Callosum	0.49 ± 0.05	0.56 ± 0.05	<0.001	1.40
L Anterior Cerebellar Peduncle	0.35 ± 0.04	0.39 ± 0.04	<0.001	1.00
R Anterior Cerebellar Peduncle	0.35 ± 0.03 %	0.39 ± 0.03	<0.001	1.33
Brain regions with increased FA in SVHD				
L Cerebellum	0.21 ± 0.02	0.19 ± 0.02	<0.001	1.00
R Cerebellum	0.22 ± 0.02	0.20 ± 0.02	<0.001	1.00
L Posterior Cerebellar Peduncle	0.40 ± 0.02	0.38 ± 0.02	<0.001	1.00
L Posterior Insula	0.22 ± 0.02	0.20 ± 0.02	<0.001	1.00
R Posterior Insula	0.22 ± 0.02	0.20 ± 0.02	0.002	1.00
L Prefrontal Cortex	0.23 ± 0.04	0.20 ± 0.04	<0.001	0.75
R Prefrontal Cortex	0.23 ± 0.04	0.19 ± 0.04	<0.001	1.00
L Putamen	0.28 ± 0.02	0.26 ± 0.02	<0.001	1.00
R Putamen	0.27 ± 0.02	0.25 ± 0.02	<0.001	1.00

SVHD, Single Ventricle Heart Disease; L, Left; R, Right; WM, White matter.